

## A probabilistic aggregation kernel for the computer-simulated transition from DLCA to RLCA

G. ODRIOZOLA(\*), A. MONCHO-JORDÁ, A. SCHMITT, J. CALLEJAS-FERNÁNDEZ,  
R. MARTÍNEZ-GARCÍA and R. HIDALGO-ÁLVAREZ(\*\*)

*Grupo de Física de Fluidos y Biocoloides, Departamento de Física Aplicada  
Universidad de Granada - Campus de Fuentenueva, E-18071 Granada, Spain*

(received 7 August 2000; accepted in final form 15 January 2001)

PACS. 82.70.Dd – Colloids.

PACS. 82.40.Bj – Oscillations, chaos, and bifurcations.

PACS. 02.50.-r – Probability theory, stochastic processes, and statistics.

**Abstract.** – A simple sticking probability model is used for deducing a kernel capable to describe the kinetics of computer-simulated irreversible aggregation processes. Not only the diffusion- and reaction-limited aggregation regimes were fitted but also the whole transition region. The deduced kernel establishes  $\lambda = 0$  for the entire range of sticking probabilities and helps to understand how irreversible cluster-cluster aggregation works.

Aggregation phenomena occur in a wide variety of physical, chemical and biological processes [1]. The stage of aggregation for a given system may be characterized by the cluster size distribution,  $\vec{N} = (N_1, N_2, \dots, N_i, \dots)$ , where  $N_i$  denotes the number of  $i$ -size clusters. For irreversible aggregation processes in diluted systems, the time evolution of the probability,  $P(\vec{N}, t)$ , for finding the system in a given state,  $\vec{N}$ , is given by the non-deterministic master equation [2, 3]

$$\frac{dP(\vec{N}, t)}{dt} = \frac{1}{2V} \sum_{i,j} k_{ij} [(N_i + 1)(N_j + 1 + \delta_{ij})P(\vec{N}_{ij}^*, t) - N_i(N_j - \delta_{ij})P(\vec{N}, t)], \quad (1)$$

where  $V$  is the volume of the system and  $\vec{N}_{ij}^*$  is defined as

$$\vec{N}_{ij}^* = \begin{cases} (\dots, N_i + 1, \dots, N_j + 1, \dots, N_{i+j} - 1, \dots) & \text{for } i \neq j, \\ (\dots, N_i + 2, \dots, N_{2i} - 1, \dots) & \text{for } i = j. \end{cases}$$

All physical information about the aggregation mechanism is contained in the kernel,  $k_{ij}$ , which quantifies the mean aggregation rate for a pair of  $i$ - and  $j$ -size cluster.

Initial studies were concerned principally with the diffusion-limited cluster aggregation regime (DLCA) where the clusters diffuse freely and form a new bond as soon as they collide.

---

(\*) Permanent address: Departamento de Química Física y Matemática, Facultad de Química, Universidad de la República - 11800 Montevideo, Uruguay.

(\*\*) E-mail: rhidalgo@ugr.es

The DLCA kinetics is well described by the Brownian kernel which was derived by considering the fractal nature of the clusters. DLCA experiments and computer simulations yield a fractal dimension closed to 1.75 and  $\lambda = 0$  [4, 5]. Here,  $\lambda$  is the homogeneity exponent defined by the relationship,  $k_{ai,aj} \sim a^\lambda k_{ij}$ , for large cluster sizes where  $a$  is a positive constant [6]. Experimental and computer-simulated data agree perfectly with the Brownian kernel solutions. The analytical expression for this kernel is  $k_{ij} = (k_{11}^{\text{Sm}}/4) (i^{1/d_f} + j^{1/d_f}) (i^{-1/d_f} + j^{-1/d_f})$ , where  $k_{11}^{\text{Sm}} = 8kT/3\eta$  is the Smoluchowski dimer formation rate constant.  $kT$  is the thermal energy,  $\eta$  is the solvent viscosity and  $d_f$  is the cluster fractal dimension. According to its definition, the Brownian kernel has  $\lambda = 0$ . It may be written as  $k_{ij} \sim (t_{\text{dif}})^{-1}$ , where  $t_{\text{dif}}$  represents the average diffusion time spent by two  $i$ - and  $j$ -size clusters before they collide.

Reaction-limited cluster aggregation (RLCA) occurs when a large number of cluster-cluster collisions is needed before a bond is formed. From experiments and computer simulations, a fractal dimension of 2.1 is commonly obtained for this regime [7]. Nevertheless, a wide range of values for the homogeneity exponent  $\lambda$  is reported in the literature. These values fall usually between 0.5 and 1 [3, 5, 7, 8]. For sufficiently large aggregation times,  $\lambda$  is related to the weight-average cluster size,  $\bar{n}_w = \sum_{i=1}^{\infty} i^2 N_i / \sum_{i=1}^{\infty} i N_i$ , by  $\bar{n}_w \sim t^{1/(1-\lambda)}$ . So,  $\bar{n}_w$  grows linearly with time for  $\lambda = 0$  and faster than linear for  $\lambda > 0$ . Since aggregation rates may not exceed the DLCA values, this average can never surpass the limit given by the curve having  $\lambda = 0$ . Hence, a true asymptotic behaviour having  $\lambda > 0$  is non-physical. The only sense in which RLCA is said to have higher  $\lambda$  than in DLCA is in the sense of a crossover [7, 9, 10].

For further discussion, it is convenient to distinguish between cluster-cluster collision and cluster-cluster encounter. In this work, we call ‘‘collision’’ the event ‘‘two cluster touch each other’’ and define ‘‘encounter’’ as a sequence of consecutive collisions between a given pair of clusters. This means that an encounter starts with the first collision and ends when the clusters aggregate or diffuse away. So, a cluster spends an average time  $t_{\text{dif}}$  between two consecutive encounters and an average time  $t_c$  between two consecutive collisions.

Ball *et al.* proposed a kernel for describing the RLCA kinetics of fractal clusters and determined its functional form by scaling arguments [10]. Nevertheless, empiric expressions like the sum kernel,  $k_{ij} = k_{11}(i^\lambda + j^\lambda)/2$ , or the product kernel,  $k_{ij} = k_{11}(ij)^{\lambda/2}$  [3, 11], are still used as fair approximations. Physically deduced kernels for the whole range of sticking probabilities are so far not known. This is, at least partially, due to the fact that it is not clear how an aggregation process occurs in detail. This can easily be understood by considering that a cluster, which needs a fixed number of collisions before forming a bond, could be involved in a small or a large number of encounters. The time required for this particular aggregation process may be quite different in both cases. So, some questions arise: What is the average number of collisions per encounter? Is this number fixed or is it a function of the cluster size? May the possible answer explain why larger clusters are more reactive than smaller ones? In this letter, we propose a simple probabilistic model which allows us to deduce an aggregation kernel and to address these questions quantitatively.

The proposed aggregation kernel is based on the expression  $k_{ij} \sim \langle t \rangle^{-1}$ , where  $\langle t \rangle$  is the average time spent by a pair of  $i$ - and  $j$ -size clusters before aggregation. The clusters are considered to move by Brownian motion and to collide after an average diffusion time  $t_{\text{dif}}$ . Generally, not every collision leads to aggregation, and so a sticking probability  $P$  must be defined. Consequently,  $(1 - P)$  is the probability for a collision which does not lead to the formation of a new bond. If the clusters aggregate immediately, then they spend an average time  $t_{\text{dif}}$  for the whole process. If they do not, they may collide again or diffuse away in order to collide with a third cluster. Hence, it is convenient to define  $P_c$  as the probability for the clusters to collide again. Consequently, the probability for the clusters to diffuse away, *i.e.*

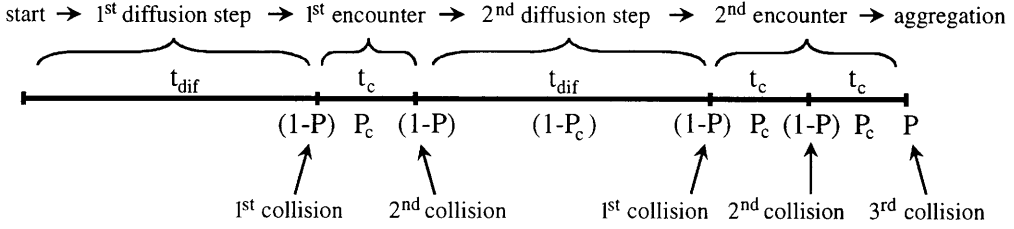


Fig. 1 – Schematic time and probability diagram for the particular aggregation process described in the text.

to quit an encounter without forming a new bond, is given by  $(1 - P_c)$ . Since the collision cross-section grows with cluster size, one expects that the bigger the clusters are the bigger  $P_c$  becomes. As an example for a more complex aggregation process, the following event may be considered: “Two clusters diffuse and collide two times. Then one of them diffuses away and collides three times with a third cluster before forming a new bond”.

Figure 1 shows a schematic time and probability diagram for this particular process. The average time for this event is  $t_{ev} = 2t_{dif} + 3t_c$  since it consists of two encounters with two and three consecutive collisions, respectively. The corresponding probability is given by  $P_{ev} = P(1 - P)^4(1 - P_c)P_c^3$ . In order to determine the average aggregation time  $\langle t \rangle$ , it is necessary to consider the duration of all possible events weighted by the corresponding probability. Hence,  $\langle t \rangle = \sum_{ev} t_{ev}P_{ev}$  may be expressed as

$$\langle t \rangle = \sum_{n=1}^{\infty} \sum_{k=0}^{n-1} \binom{n-1}{k} [(n - k)t_{dif} + kt_c] P(1 - P)^{n-1} P_c^k (1 - P_c)^{n-1-k}. \quad (2)$$

Using the well-known solutions for geometrical and binomial series, eq. (2) becomes finally

$$\langle t \rangle = \frac{t_{dif} + (t_c - t_{dif})(1 - P)P_c}{P}. \quad (3)$$

As expected, the above expression leads to the Brownian kernel for  $P = 1$ . For  $P < 1$ , the kernel gives smaller rate constants for all cluster sizes.

The probability  $P_c$  is related to the mean number of collisions per encounter for a non-aggregating system. According to its definition, this quantity is given by  $\mathcal{N} = \sum_{i=1}^{\infty} iP_c^{(i-1)}(1 - P_c) = 1/(1 - P_c)$ . As mentioned above, it is reasonable to allow  $\mathcal{N}$  to be size dependent. Since the dependency must be a symmetric function of the cluster sizes  $i$  and  $j$ , we assume  $\mathcal{N}_{ij} = \mathcal{N}_{11}(ij)^b$ . Here,  $\mathcal{N}_{11}$  is the mean number of monomer collisions per encounter and  $b$  a constant. For diluted systems, the average collision time,  $t_c$ , should be much smaller than the average diffusion time,  $t_{dif}$  and so may be neglected in the  $(t_c - t_{dif})$  term. Substituting  $P_c$  in eq. (3) and assuming  $(t_c - t_{dif}) \approx -t_{dif}$ , leads finally to

$$k_{ij} = \frac{k_{11}^{Sm} (i^{1/d_f} + j^{1/d_f})(i^{-1/d_f} + j^{-1/d_f}) P \mathcal{N}_{11}(ij)^b}{4(1 + P[\mathcal{N}_{11}(ij)^b - 1])}. \quad (4)$$

For large cluster sizes, this kernel approaches the Brownian kernel, and so has  $\lambda = 0$  for all sticking probabilities. This finding is in excellent agreement with the theoretical prediction that after a sufficiently large time, irreversible aggregation should always reach the diffusion-limited aggregation regime [12].

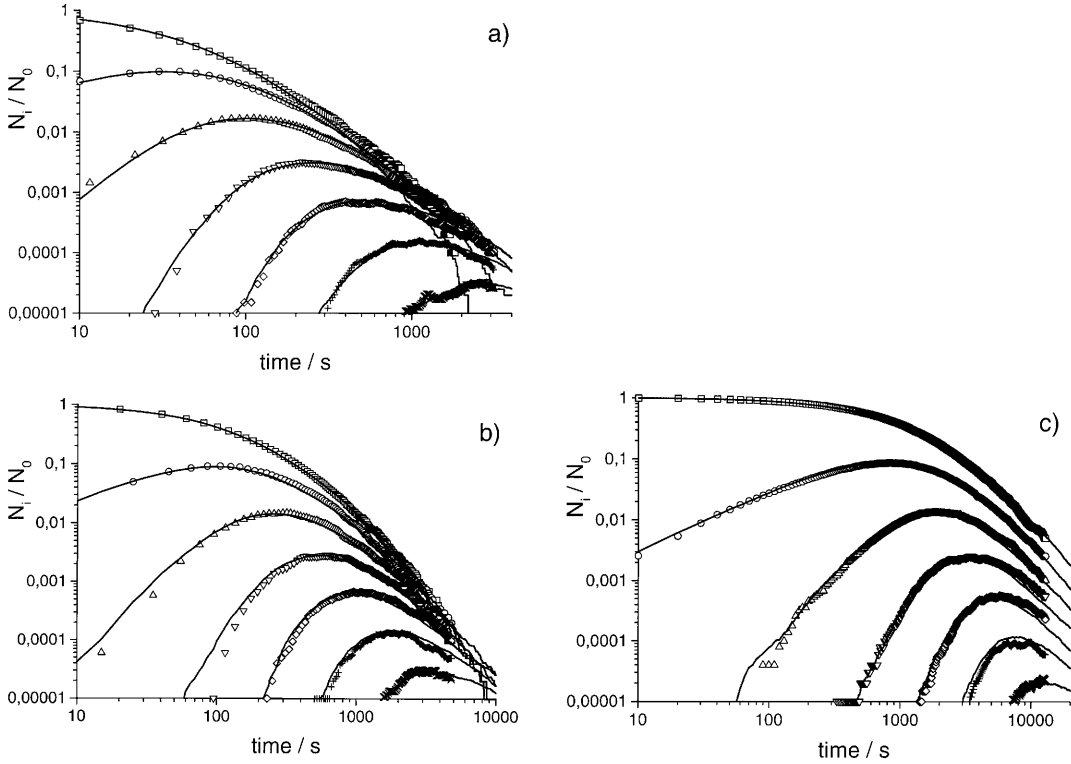


Fig. 2 – Time evolution of the normalized cluster size distribution for the sticking probabilities a) 0.5, b) 0.05, and c) 0.005. The points correspond to the computer-simulated data for monomers up to 200-mers grouped in logarithmically spaced intervals ( $\square$  monomers,  $\circ$  2- and 3-mers,  $\triangle$  4- to 8-mers,  $\nabla$  9- to 18-mers,  $\diamond$  19- to 38-mers,  $+$  39- to 88-mers and  $\times$  89- to 200-mers). The solid lines represent the corresponding stochastic solutions for the proposed kernel.

In order to test the validity of the derived kernel, we confront the corresponding solutions with simulated data and compare the results also with the Brownian, sum and product kernel. The simulations were performed in 3 dimensions, off-lattice and with periodical boundary conditions. A volume fraction of  $5.0 \times 10^{-4}$  and a step length of 0.5 times the particle radius was set. The simulated aggregation processes started always from monomeric initial conditions for a total number of  $N_0 = 10^4$  particles. In order to convert the simulation time into real time, the monomer diffusivity has to be given. This parameter was arbitrarily chosen to be  $D_1 = 6.8 \times 10^{-13} \text{ m}^2\text{s}^{-1}$ . The simulations were carried out for the sticking probabilities 1, 0.5, 0.1, 0.05, 0.01 and 0.005. The cluster fractal dimension was determined using the radius of gyration method described in ref. [13].

For solving eq. (1), the stochastic algorithm described in refs. [2] and [3] was used. For this purpose, the same volume fraction and monomeric initial conditions as set for computer simulations were established. The number of initial particles was set to  $N_0 = 10^5$  in order to achieve reliable statistics. As aggregation kernel, the expression given by eq. (4) was used. This kernel is a function of  $k_{11}^{\text{Sm}}$ ,  $P$ ,  $d_f$ ,  $\mathcal{N}_{11}$  and  $b$ . Here,  $k_{11}^{\text{Sm}}$  was calculated from the theoretical expression  $k_{11}^{\text{Sm}} = 8kT/3\eta$ . This yields  $k_{11}^{\text{Sm}} = 11.1 \times 10^{-18} \text{ m}^3\text{s}^{-1}$  for aqueous systems at 293 K.  $P$  is, as input value, known from the simulations. As mentioned above,  $d_f$  was determined directly from the structure of the simulated clusters.  $\mathcal{N}_{11}$  was assessed by

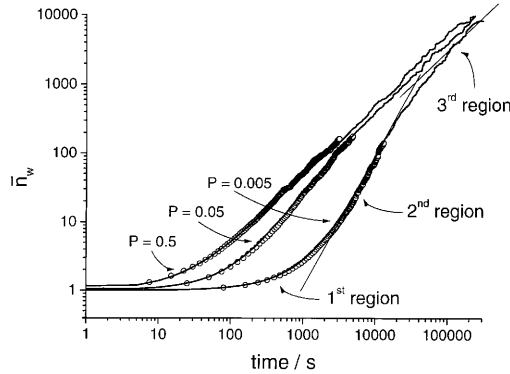


Fig. 3 – The time evolution of the weight-average cluster size,  $\bar{n}_w$ , calculated for different sticking probabilities. The points correspond to the computer-simulated data. The solid lines represent the corresponding stochastic solution for the proposed kernel.

averaging the number of consecutive collisions for all pairs of particles during a simulation run with  $P = 0$ . Under the given simulation conditions,  $\mathcal{N}_{11} = 6.1$  was obtained. Hence,  $b$  is the only undetermined parameter.

Figure 2 shows the time evolution of the simulated cluster size distribution for the sticking probabilities 0.5, 0.05 and 0.005 together with the corresponding stochastic solution of the master equation. In all cases, an excellent agreement is observed. The same happens for the sticking probabilities 1, 0.1 and 0.01 which are not included in the plot. It should be pointed out that the same  $b$  value was used for the complete set of theoretical solutions. The best fits were obtained for  $b = 0.35$ . Please note that no fitting parameter was needed for the DLCA limit. This means that the theoretical Smoluchowski dimer rate constant is naturally obtained from the simulations.

Figure 3 shows the time evolution of the average cluster size,  $\bar{n}_w$ , for different sticking probabilities. Also here, an excellent agreement between the simulated data and the stochastic solutions is observed. For all curves, three well-defined regions may be distinguished. For short times,  $\bar{n}_w$  starts from unity and, as expected, grows faster for larger sticking probabilities. At intermediate times, an apparent asymptotic behaviour appears and remains up to relatively long aggregation times. In this region,  $\bar{n}_w$  reaches quite large values. The  $\lambda$  values, reported in the literature, are usually obtained from this region. Please note that the slopes of the curves increase for decreasing sticking probabilities. In the limiting case of  $P \rightarrow 0$ , a slope of  $1/(1 - 2b)$  is expected. The third region corresponds to very long times and extremely large cluster sizes. Here, all curves approach the same real asymptotic behaviour where  $\lambda$  becomes 0. As can be seen, the curves for different sticking probabilities  $P$  never cross the limiting DLCA curve. So, the proposed kernel predicts an asymptotic large-time behaviour consistent with theoretical considerations. This region is, however, very difficult to achieve in experiments and simulations due to the extremely large size of the corresponding clusters.

In order to quantify the quality of the fits and to allow for comparison with other kernels, we define  $Err = (\sum_{j=1}^7 \sum_{i=1}^a \xi_{ij}^2 / 7a)^{1/2}$  as the square root of the relative mean quadratic deviation between the numerical solutions and the data. Here,  $\xi_{ij}$  is the relative deviation between the data point number  $i$  of curve number  $j$  and the corresponding numerical solution.  $a$  is the number of data points per curve. As can be seen in table I the  $Err$  values for the proposed kernel are always very small and independent of the sticking probability  $P$ . This

TABLE I – Fitting parameters and *Err* values for the different kernels used for describing the simulated data. The dimer formation rate constants,  $k_{11}$ , are given in units of  $10^{-18} \text{ m}^3\text{s}^{-1}$ .

$P$	Proposed kernel		Brownian kernel		Sum kernel			Product kernel		
	$b$	<i>Err</i>	$k_{11}$	<i>Err</i>	$k_{11}$	$\lambda$	<i>Err</i>	$k_{11}$	$\lambda$	<i>Err</i>
1	–	0.155	11.1	0.155	13.0	0.00	0.165	13.0	0.00	0.165
0.5	0.35	0.172	10.0	0.192	11.0	0.05	0.184	11.0	0.05	0.201
0.1	0.35	0.165	5.0	0.388	5.0	0.25	0.224	5.0	0.25	0.236
0.05	0.35	0.151	3.0	0.562	3.0	0.35	0.277	3.0	0.35	0.305
0.01	0.35	0.158	0.70	3.02	0.70	0.55	0.195	0.70	0.55	0.273
0.005	0.35	0.167	0.35	3.20	0.35	0.60	0.172	0.35	0.60	0.175

means that it fits the RLCA limit and the complete transition region with the same high degree of accuracy as the DLCA regime.

Now, we use the *Err* values to compare the fits with the Brownian, the sum and the product kernel solutions. For the Brownian kernel,  $k_{11}$  was employed as the only free parameter for fitting the initial steps of aggregation. As expected, the corresponding solution naturally describes the complete time evolution for  $P = 1$ . In this case,  $k_{11}$  matches the theoretical Smoluchowski value. For slower processes, however, the agreement worsens drastically (see table I). The sum and the product kernel have  $k_{11}$  and  $\lambda$  as free parameters. Also here,  $k_{11}$  was used for fitting the onset of aggregation.  $\lambda$  was then varied to match the long-time behaviour of  $\bar{n}_w$ . For both kernels and all sticking probabilities, it was possible to fit the  $\bar{n}_w$  curves perfectly. The detailed cluster size distribution, however, could be reproduced only for small and large sticking probabilities. In the intermediate region, the *Err* values increase approximately by a factor of two. Figure 4 shows the sum kernel fit for  $P = 0.05$ . Here, it can be clearly seen that matching the  $\bar{n}_w$  curves is not sufficient for guaranteeing an adequate fit of the detailed cluster size distribution. It should be pointed out that, even with two free adjustable parameters, neither the sum nor the product kernel are able to describe the complete DLCA-RLCA transition. On the contrary, the proposed kernel is capable to fit the whole transition with high accuracy and only one global parameter which does not depend on the sticking probability  $P$ . This means that the assumptions made for deducing the proposed kernel are reasonable and sufficient for describing irreversible aggregation processes.

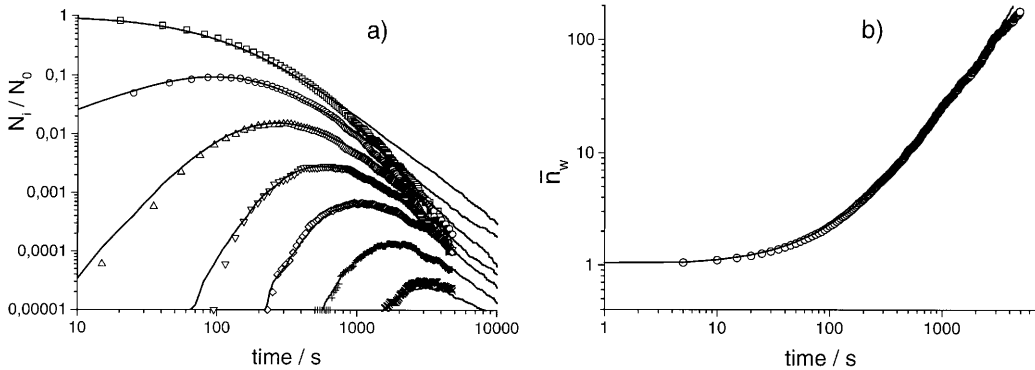


Fig. 4 – a) Time evolution of the normalized cluster size distribution for  $P = 0.05$ . Just like in fig. 1b), the points correspond to the computer-simulated data while the solid lines represent the best fit for the sum kernel. b) Time evolution of the corresponding weight-average cluster size  $\bar{n}_w$ .

The proposed probabilistic aggregation model allows even to draw some additional conclusions. For example, the positive value obtained for  $b$  shows that the average number of collisions per encounter,  $\mathcal{N}_{ij}$ , increases for increasing cluster size. As mentioned above,  $\mathcal{N}_{11} = 6.1$  was obtained. This means that, under the given simulation conditions, the monomers collide on average 6.1 times per encounter. So, for a sticking probability of 0.01, where the clusters need an average of 100 collisions for forming a bond, the monomeric particles are involved in 16.4 encounters and consequently, spend an average time of  $16.4t_{\text{dif}} + 73.6t_c$  for aggregation. Decamers, however, will collide among themselves  $\mathcal{N}_{10\ 10} = 27.9$  times per encounter and so spend an average time of  $3.6t_{\text{dif}} + 96.4t_c$ . Given that  $t_c \ll t_{\text{dif}}$ , it becomes clear why decamers are more reactive than monomers. In the limiting case of very large cluster sizes, only one encounter is expected and so the cluster reactivities approach the DLCA values.

In conclusion, the proposed probabilistic model helps to understand how irreversible cluster-cluster aggregation works. It gives rise to a physically deduced kernel which reproduces the time evolution of the cluster size distributions for all times, cluster sizes and sticking probabilities. This fact confirms that the presented model is capable to describe the transition from DLCA to RLCA. It also gives a plausible explanation for the apparent DLCA-RLCA  $\lambda$  contradiction mentioned at the beginning of this letter and establishes  $\lambda = 0$  for the real asymptotic behaviour of irreversible aggregation processes.

\* \* \*

This work was supported by the *Comisión Interministerial de Ciencia y Tecnología* (CICYT, Project MAT97-1024). GO is grateful for a scholarship granted by the *European Union* (Program: *alfa*, proposal No. ALR / B7-3011 / 94.04-6.017.9). AS is grateful for financial support from the *Gottlieb Daimler- and Karl Benz-Stiftung*.

## REFERENCES

- [1] DHONT J. K. G., *An Introduction to Dynamics of Colloids* (Elsevier, Amsterdam) 1996; HIDALGO-ÁLVAREZ R., MARTÍN A., FERNÁNDEZ-BARBERO A., BASTOS D., MARTÍNEZ F. and DE LAS NIEVES F. J., *Adv. Colloid Interface Sci.*, **67** (1996) 1.
- [2] GILLESPIE D. T., *J. Phys. Chem.*, **81** (1977) 2340.
- [3] THORN M. and SEESSELBERG M., *Phys. Rev. Lett.*, **72** (1994) 3622.
- [4] WEITZ D. A., HUANG J. S., LIN M. Y. and SUNG J., *Phys. Rev. Lett.*, **53** (1984) 1657; BROIDE M. L. and COHEN R. J., *Phys. Rev. Lett.*, **64** (1990) 2026; *J. Colloid Interface Sci.*, **153** (1992) 493; ODRIOZOLA G., SCHMITT A., CALLEJAS-FERNÁNDEZ J., MARTÍNEZ-GARCÍA R. and HIDALGO-ÁLVAREZ R., *J. Chem. Phys.*, **111** (1999) 7657.
- [5] MEAKIN P. and FAMILY F., *Phys. Rev. A*, **36** (1987) 5498.
- [6] VAN DONGEN P. G. J. and ERNST M. H., *Phys. Rev. Lett.*, **54** (1985) 1396; *J. Stat. Phys.*, **50** (1987) 295.
- [7] LIN M. Y., LINDSAY H. M., WEITZ D. A., BALL R. C., KLEIN R. and MEAKIN P., *Phys. Rev. A*, **41** (1990) 2005.
- [8] OLIVER B. J. and SORENSEN C. M., *J. Colloid Interface Sci.*, **134** (1990) 139.
- [9] FAMILY F., MEAKIN P. and VICSEK T., *J. Chem. Phys.*, **83** (1985) 4144.
- [10] BALL R. C., WEITZ D. A., WITTEN T. A. and LEYVRAZ F., *Phys. Rev. Lett.*, **58** (1987) 274.
- [11] DI BIASIO A., BOLLE G., CAMETTI C., CODASTEFANO P., SCIORTINO F. and TARTAGLIA P., *Phys. Rev. E*, **50** (1994) 1649; CALOGERO F. and LEYVRAZ F., *J. Phys. A*, **32** (1999) 7697; VAN DONGEN P. G. J. and ERNST M. H., *Phys. Rev. A*, **32** (1985) 670.
- [12] VAN DONGEN P. G. J., *Phys. Rev. Lett.*, **63** (1989) 1281.
- [13] VICSEK T., *Fractal Growth Phenomena* (World Scientific, Singapore) 1992; JULLIEN R., *Croat. Chem. Acta*, **65** (1992) 215.